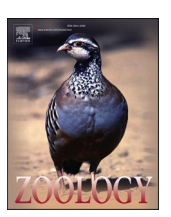


Contents lists available at ScienceDirect

# Zoology

journal homepage: www.elsevier.com/locate/zool





# Effect of parabranchial position on ventilatory pressures in the Pacific spiny dogfish (*Squalus suckleyi*)

Sarah Arnette a,b,\*, Jacob Saffarian b,d, Lara Ferry a, Stacy Farina b,c

- a New College, Department of Math and Natural Sciences, Arizona State University West, 4701 W. Thunderbird Rd, Glendale, AZ 85306, United States
- <sup>b</sup> Friday Harbor Laboratories, University of Washington, 620 University Rd, Friday Harbor, WA 92150, United States
- <sup>c</sup> Department of Biology, Howard University, 415 College St NW, Washington, DC 20059, United States
- <sup>d</sup> UC Berkeley, Rausser College of Natural Resources, 110 Sproul Hall, Berkeley, CA 94720, United States

# ARTICLE INFO

Keywords: Elasmobranch Breathing Gills

## ABSTRACT

The mechanics of ventilation in elasmobranchs have been described as a two-pump system which is dependent on the generation of differential pressures between the orobranchial and parabranchial cavities. However, this general model does not take into account sources of variation in parabranchial form and function. For example, the relative pressures that drive flow in each parabranchial chamber during ventilation remain largely unexplored. To address this gap, parabranchial pressures were collected from the Pacific spiny dogfish (Squalus suckleyi, n = 12) during routine ventilation using transducers inserted into parabranchial chambers 2, 3, and 5, numbered anteriorly to posteriorly. Pressure amplitudes collected from the three chambers displayed an attentation of pressure amplitudes posteriorly, as well as differential, modular use of parabranchial chamber five These observations have implications for the functioning of the ventilatory pump and indicate distinct ventilatory modes, leading us to propose a new model to describe ventilation in Squalus suckleyi.

# 1. Introduction

Most fishes, including actinopterygians and elasmobranchs (sharks, skates, and rays) generate a respiratory current over the gills using active (pump) ventilation. Pump ventilation is kinematically complex, using a double-pump system that involves the oral and parabranchial chambers (Hughes, 1960a; 1960b; Brainerd and Ferry-Graham, 2005). Elasmobranchs begin pump ventilation by depressing the mandible and hyoid, creating a "suction pump" of negative pressure that pulls water into the orobranchial cavity through the mouth and spiracles. The suction pump continues with the expansion of the parabranchial chambers (PBCs) creating negative pressure that pulls water across the gill filaments. The mandible is then adducted and hyoid elevated to create a positive pressure "force pump", which pushes water out of the parabranchial openings when combined with the compression of the parabranchial cavities. This alternating pull-push of water is facilitated by the expansion and compression of the parabranchial chambers, which drive flow of water into and out of the chambers. This flow is accurately determined using pressure measurement (Hughes, 1960a; 1960b; Ferry-Graham, 1999This dual pump system provides nearly continuous and

largely unidirectional flow over the gills, which enhances the efficiency of countercurrent exchange at the gill lamellae, supported by hemibranchs (Fig. 1) (Scheid et al., 1986). Sharks are well known for an alternate mechanism — ram ventilation, where ventilatory flow is generated by forward locomotion (Wegner et al., 2012; Wegner and Graham, 2010) — from which comes the popular notion that sharks must swim all the time to breathe, a condition called obligate ram ventilation. However, most species can employ pump ventilation at some times, if not all the time. Therefore, while pump ventilation is more complex, it is far more common in sharks than the ram ventilation for which they are known.

A hallmark of pump ventilation is the cyclical opening and closing of the five bilaterally paired external openings present in most elasmobranch taxa (Dolce and Wilga, 2012). These five openings often vary in size, shape, and location within and across species. This suggests that there could be differences in how each parabranchial chamber contributes to ventilatory flow, likely linked with external factors such as chamber size and location, as noted preliminarily by Hughes (1960a).

The primary goal of this study was to describe the differences in the generation of pressures in multiple parabranchial chambers and

E-mail address: sarahhandy96@gmail.com (S. Arnette).

<sup>\*</sup> Corresponding author at: New College, Department of Math and Natural Sciences, Arizona State University West, 4701 W. Thunderbird Rd, Glendale, AZ 85306, United States.

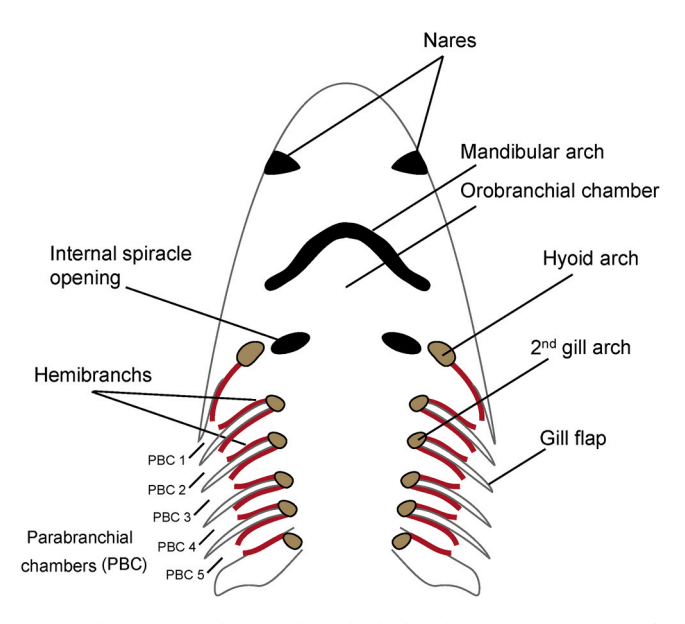


Fig. 1. Schematic of the parabranchial chamber anatomy in *Squalus suckleyi*. A ventral cross-sectional view of the general morphology of the orobranchial and parabranchial chambers (PBCs) of the dogfish, adapted from Wegner (2016).

investigate the impact of parabranchial chamber position on the generation of ventilatory pressure in *S. suckleyi*. We hypothesized that parabranchial chambers (PBCs) located more posteriorly would generate relatively lower pressure amplitudes than those located anteriorly due to the flow of water encountering friction along the gills. Due to our inability to access PBC 1 (See Methods Section 2.1), we recorded ventilatory pressures in the second, third, and fifth PBC of 12 individuals of *S. suckleyi*. Specifically, we tested the hypotheses that 1) PBC 2 would have the highest pressure amplitude and PBC 5 would have the lowest, and 2) PBC 2 would reach a pressure maximum before PBC 3 and PBC 5, indicating a phase shift in the timing of the pumps. Both pressure generation and a phase shift in timing have implications for the maintenance of unidirectional flow over the gills, which is of paramount importance for the efficiency of gas exchange.

# 2. Materials and methods

# 2.1. Specimens

A total of twelve individuals of *S. suckleyi* were included in the study (5 in 2019 and 7 in 2021) and ranged in size from 52 to 83 cm total length (tip of the rostrum to the dorsal tip of the caudal fin). Specimens were caught via both otter trawl and hook and line fishing at depths ranging from 20 to 60 m in the Salish Sea surrounding Friday Harbor Laboratories. The sharks were housed in flow-through seawater tanks with a 2.4 m diameter and 76 cm depth, with no more than four individuals per tank at one time. Sharks were fed a diet of frozen herring and shrimp every 2–3 days, based on their willingness to eat; they were fasted for 72 h prior to experimentation to ensure a post-absorptive state. Individuals were permitted to acclimate to captivity for at least 4 days prior to beginning any experiments; all experiments were conducted under University of Washington's IACUC protocol 4238–03.

Prior to live animal work, a freshly frozen shark was dissected to examine the underlying branchial musculature and vasculature to ensure placement of the pressure transducers would produce minimal damage in the live, anesthetized individuals. We observed extensive musculature external to PBC 1, which would have been unavoidably damaged by the implantation process, thereby interfering with normal ventilatory movements. Parabranchial chambers 2–5, numbered

anterior to posterior, did not possess this underlying elaboration, leading us to choose PBC 2, 3, and 5 for implantation as illustrated by Fig. 2. PBC 5 was of particular interest, as obvious reductions in movement at this opening compared with the other four openings were observed during our routine observations of the sharks prior to experimentation.

To implant the cannulae and pressure transducers, individuals were anesthetized using tricaine methanesulfonate (MS-222) in seawater at 110 mg/L (Popovic et al. 2012). Intraparabranchial pressure data were collected using Millar Mikro-tip SPR 524 pressure transducers. Prior to placing the pressure transducers, we placed PE 90 polyethylene cannulas into PBCs 2, 3, and 5 using a 15-gauge needle to pierce the epithelium at the dorsal portion of the gill flap where it separates from the body wall (Fig. 1B). Prior to the insertion of the cannulae, we used a warm soldering iron to flare the ends that would reside inside the parabranchial chamber to ensure that it would lay flush with the interior surface of the parabranchial chamber but would not pull out. Then, approximately 8 cm of tubing was threaded through each hole, such that the flared end lay flush inside the gill epithelium and the remainder of the tubing was external to the shark's body. After the three cannulae were in place, the transducers were threaded through such that the tip of the transducer was flush with the opening of the cannula, and the cannulae were checked for air bubbles and flushed to remove any that were present. Once the implantations were in place and secure, the individual was carefully moved to the recovery tank where pressure data were collected.

# 2.2. Pressure data

Pressure was recorded from individuals immediately following their placement in a  $122~\rm cm \times 48~cm \times 33~cm$  glass recording tank, where they were housed for the remainder of the data collection process. The recording chamber was filled with fresh seawater from the flow-through system at approximately  $12~\rm ^{\circ}C$ . Individuals were recorded in the experimental tank for at least thirty minutes, a period long enough to span recovery from anesthesia as well as normal ventilatory behavior; recovery from deep anesthesia to regular breathing behavior took about 15 min for all individuals. For most of the duration of the experiments, the dogfish rested on the bottom of the experimental container, breathing quiescently. However, there were some bursts of uncoordinated and/or vigorous activity, particularly when the individual was recovering from anesthesia. These periods of post-anesthesia activity were recorded, but only periods of quiescent breathing were included in the analysis.

For data collected in 2019, pressures were recorded from the Millar pressure transducers to the computer using the LabJack T7 pro and LabJack computer application. Recordings were taken at a frequency of 30 Hz. Our data collection system was moderately affected by ambient electrical noise, leading us to place the pressure transduction units in a grounded metal toolbox. For data collected in 2021, pressure was recorded using Millar pressure transducers and recorded to a computer using ADinstruments eight-channel PowerLab and the associated computer application LabChart. Recordings were taken at a frequency of 1000 Hz (1 observation per millisecond). The data collected from 2021 were used, in part, to validate the data collected in 2019 prior to including data from both sampling years.

The following variables were extracted from the combined dataset: pressure maximum (the point at which pressure is greatest in the PBC), pressure minimum (when pressure is lowest in the PBC), and pressure amplitude (the difference between pressure maxima and minima). All pressure measurements, including maxima, minima, and pressure amplitude, were measured in voltage and converted to Pascals (Pa) by two-point calibration. We also collected the time associated with maximum pressure (when the parabranchial chamber is closed) and minimum pressure (when the parabranchial chamber is fully open) in milliseconds. Ventilatory frequency is reported in Hertz (Hz) for breaths per second. The total length (cm) of each shark was also included as a

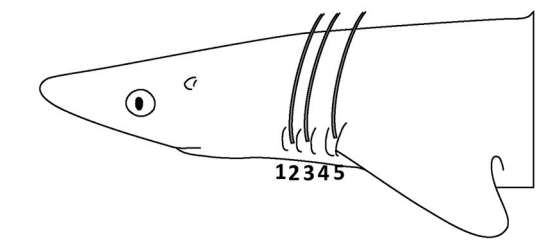




Fig. 2. (A) A schematic illustrating the insertion of cannula through the epithelium of the second, third, and fifth parabranchial chambers (PBCs) numbered anteriorly to posteriorly. (B) Photograph of an experimental individual indicating the placement of the cannula and pressure transducers.

variable.

# 2.3. Statistical analysis

We analyzed 60 breaths from 12 individuals (20 consecutive breaths from three non-consecutive sequences chosen at random from each individual), for a total of 720 breaths. The selected sequences were chosen to span the breadth of the data collection period, with 10-20 min between each sequence. To account for ambient noise, the data were filtered (3rd degree, frequency =0.15 Hz) using a backwards and forwards Butterworth filter with the *filtfilt* function of the *signal* package in R (R Core Team, 2021). We wrote a for-loop in R to obtain the amplitudes from raw data and the resultant amplitudes collected became the dataset used for all linear models.

To determine if our data were affected by shark length, we used a simple linear regression with amplitude (Pa) as the dependent variable and length of shark (cm) as the independent variable. A separate regression was performed for each PBC. The residuals of these models represented a normal and size-corrected transformation of raw amplitude data and became the dataset for the ANOVA.

To test our hypothesis that amplitude decreases with position of the PBC, we used a one-factor ANOVA. The variables included in the model were the amplitude residuals from the aforementioned linear regression with amplitude and body length, and parabranchial chamber number. Breath was initially included as a repeated measures (RM) error term because we had three observations (PBC 2, 3, and 5); however, there was no difference in results when comparing between the ANOVA with and without a RM error term. Thus, we chose the simple one-factor ANOVA to facilitate the post-hoc analysis. A Tukey post-hoc test was used to check for differences between individual PBC pairings, thus finally addressing the hypothesis that pressure decreases with posterior positioning of the PBC. The ANOVA was performed in RStudio version 4.1.3 using the base function aov(). To ensure there were no confounding statistical effects that might arise from pooling sequences where PBC 5 is off and sequences where PBC 5 is on together, the ANOVA for differences between PBCs was conducted using only sequences in which the maximum amplitude in PBC 5 was greater than 50 Pa. Using this method of separating the modes, we are able to estimate how frequently the quiet mode occurs in our sample.

A linear regression was also used to determine if ventilation rate (Hz) changed with length (cm). This model included only one PBC, since ventilatory rate is the same among all chambers. The linear regressions were performed using the base function lm in RStudio.

To test the hypothesis that there would be phase shift in the timing of parabrachial expansion, with posterior chambers opening sooner, we sequestered the same sequence of twenty breaths from each PBC, and overlayed their pressure traces in RStudio. We assessed phase shift of the movements by digitizing the gill flaps of one individual filmed using a high-speed video.

#### 3. Results

# 3.1. Pressure and frequency related to size

A linear regression was used to determine if pressure amplitude changed with body length and revealed a positive and significant relationship for each of the parabranchial chambers ( $R_{PBC2}^2=0.17,\,p<0.001,\,R_{PBC3}^2=0.20,\,p<0.001,\,R_{PBC5}^2=0.19,\,p<0.001)$  (Fig. 3). The residuals of each linear regression became a size corrected, normally distributed data set for the following ANOVA analysis. A second linear regression between body length and average frequency (average number of breath cycles per second) showed that frequency generally decreased with increasing body length, but the relationship is not significant ( $R^2=0.01,\,p=0.29$ ).

# 3.2. Pressure related to parabranchial chamber position

The pressure amplitude residuals from each PBC were significantly different from one another (n = 720 breaths, df = 2, F = 1165, p < 0.001). The post-hoc Tukey test revealed that amplitudes between each pair of parabranchial chambers were also significantly different from one another ( $p_{PBC2-PBC3} < 0.001$ ,  $p_{PBC2-PBC5} < 0.001$ ,  $p_{PBC3-PBC5} < 0.001$ ). Ultimately, we determined that PBC pressure amplitudes decreased anteriorly to posteriorly (Fig. 4).

# 3.3. Behavioral observations

Although all measurements included in the analyses were collected from individuals that were fully recovered from anesthesia and resting on the bottom of the experimental chamber, we note that ventilatory amplitude and frequency were observed to be consistently higher during the recovery period. Recovery from anesthesia was also often marked with erratic swimming behavior (starting and stopping quickly, abrupt directional changes). During routine ventilation post-recovery, we observed that there appeared to be two different ventilatory modes: one "active" mode in which PBC 5 retains positive amplitude, albeit smaller than PBCs 2 and 3, and a second "quiet" mode in which there is no change in pressure in the fifth PBC (Fig. 5). We found that quiet breathing is a fairly pervasive behavior, with an average of one sequence per individual being below the 50 Pa threshold; for more information, see Supplemental Data. In both active and quiet breathing, the movement in PBC 5 appears to be reduced compared to the anterior openings; at no point was a total cessation in the movement of the external gill flap of PBC 5 observed. No phase shift in the timing of pressure changes or external movements of the gill flaps was detected.

# 4. Discussion

Pressure amplitudes decreased posteriorly among the parabranchial chambers. In all twelve individuals, amplitude was lower in the third parabranchial chamber than the second, and the fifth parabranchial chamber had the lowest measured amplitude (Fig. 4). This is similar to the observation made by Hughes (1960b) in *Scyliorhinus canicula*.

S. Arnette et al. Zoology 159 (2023) 126106

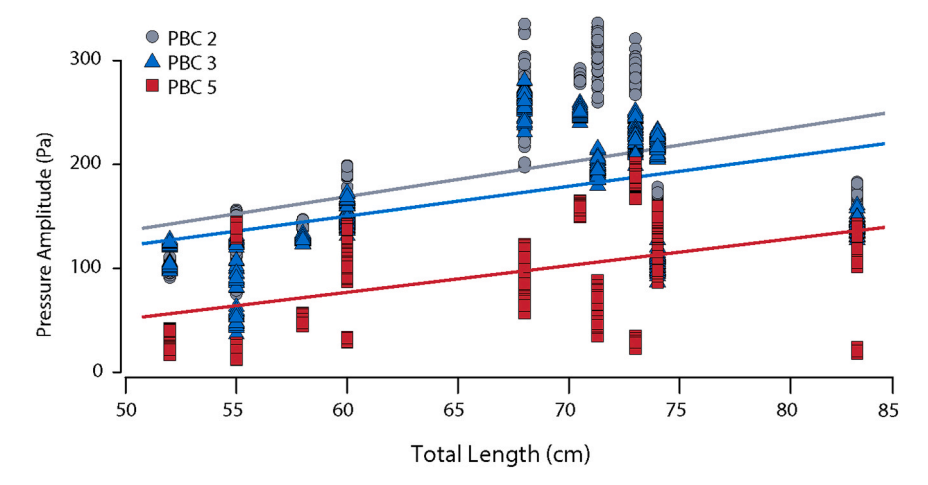


Fig. 3. Pressure amplitude and body length linear regressions by parabranchial chamber (PBC) in *S. suckleyi*. Three linear regressions indicating the relationship between generated amplitudes in each PBC and total length (n = 12).

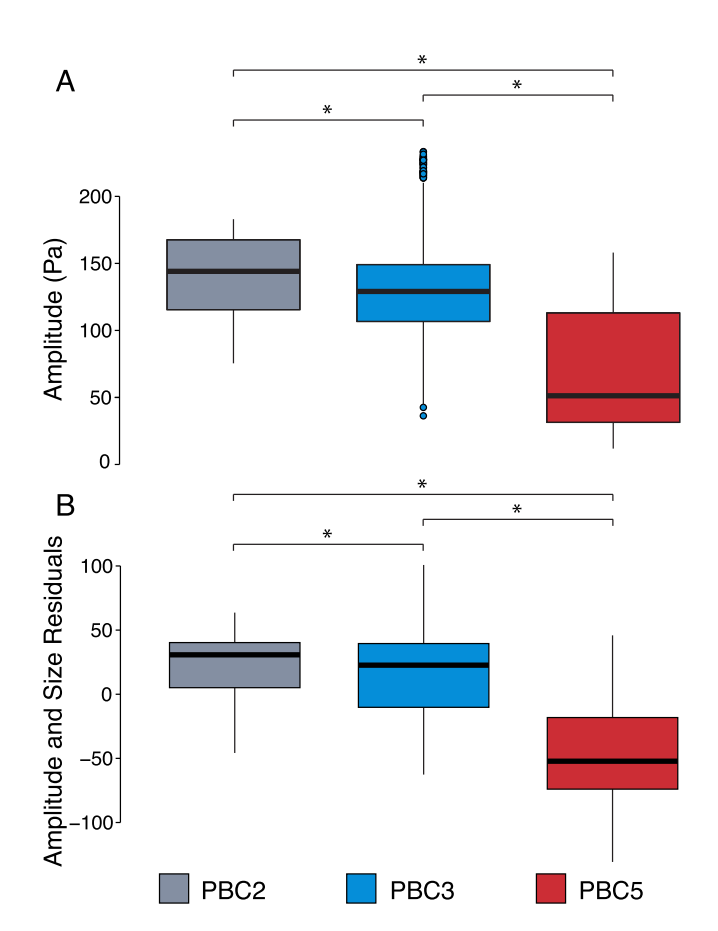


Fig. 4. Amplitude of pressures in the second, third, and fifth parabranchial chambers (PBCs) of S. suckleyi. A one-way ANOVA was conducted using parabranchial chamber as a factor. Boxplot A shows the spread of the raw, size-uncorrected amplitudes across the sampled parabranchial chambers (n=12); the heavy line represents the median amplitude, the box encompasses the quartiles above and below the median, and the whiskers encompass the minimum and maximum amplitudes, excluding outliers. There are outliers present in PBC 3. Boxplot B shows the spread of the size-corrected amplitudes, with the heavy black line representing the median and the whiskers encompassing the minimum and maximum values. There are no outliers in the size-corrected boxplots (B).

Scyliorhinids such as *S. canicula* are strongly associated with the benthos (Mytilineou et al., 2005), relative to the benthopelagic *Squalus suckleyi* (Mecklenburg et al., 2018). The discovery of differences in the parabranchial amplitudes during rest in both *S. suckleyi* and *S. canicula* given their phylogenetic distance and differences in ecology, preliminarily suggests that this may be a common occurrence among benthic and benthopelagic species of elasmobranchs.

It is likely that the lack of pressure differential observed in PBC 5 during quiet breathing is purposeful, which may be indicative of distinct ventilatory modes in S. suckleyi. This is consistent with other observations of multiple ventilation modes in the swellshark Cephloscyllium ventriosum, hedgehog skate Leucoraja erinacea, and members of the carpet shark family Parascyllidae (Ferry-Graham, 1999; Summers and Ferry-Graham, 2001; Goto et al., 2013). A model illustrating the difference between the "active" and "quiet" breathing modalities in S. suckleyi, one wherein PBC 5 is being used (active) and one where pressure in PBC 5 is near zero (quiet), is indicated by Fig. 6. Even when PBC 5 is active, it appears to generate a lower pressure than its more anterior counterparts. This is likely due to a weakening of the force pump, illustrated by the decreasing positive pressure phase (area of the curve above the zero line) in Fig. 5. During the force pump phase, a pulse of positive pressure is generated by the abduction of the mandible (Hughes, 1960b); this pulse of positive pressure then spreads posteriorly to the subsequent parabranchial cavities, where it attenuates as it encounters friction along the gills. In case 1, the "active" mode, the interbranchial resistance caused by branchial musculature is equal, so there is positive pressure generated in all five parabranchial chambers, including PBC 5. In case 2, the "quiet" mode, the interbranchial resistance is increased—likely by the complete closure of the gill flap— such that water flow through PBC 5 is entirely restricted.

Restricting the flow of water through a parabranchial chamber may serve one or more physiological purposes. *S. suckleyi* may have greater functional surface area for gas exchange than its resting metabolism demands. Many studies have suggested that fish can modulate the functional surface area for gas exchange to reduce the associated osmoregulatory costs during quiescent breathing (Booth,1978; Randall, 1970; Steen and Kruysse,1964). Additionally, there is an energetic cost to actively pumping the gills (Steffensen, Lomholt, 1983; Muir and Buckley,1967; Roberts,1975), which may be reduced by restricting flow to the posterior chambers during quiescent breathing. Quiescent breathing is quite common for benthic sharks such as the Port Jackson shark *Heterodontus portjacksoni* and the draughtsboard shark *Cephaloscyllium isabellum*, which spend a large amount of time motionless on the seafloor (Kelly et al., 2021). Some elasmobranch species have shown distinct "quiet breathing" modalities, during which the kinematics

S. Arnette et al. Zoology 159 (2023) 126106

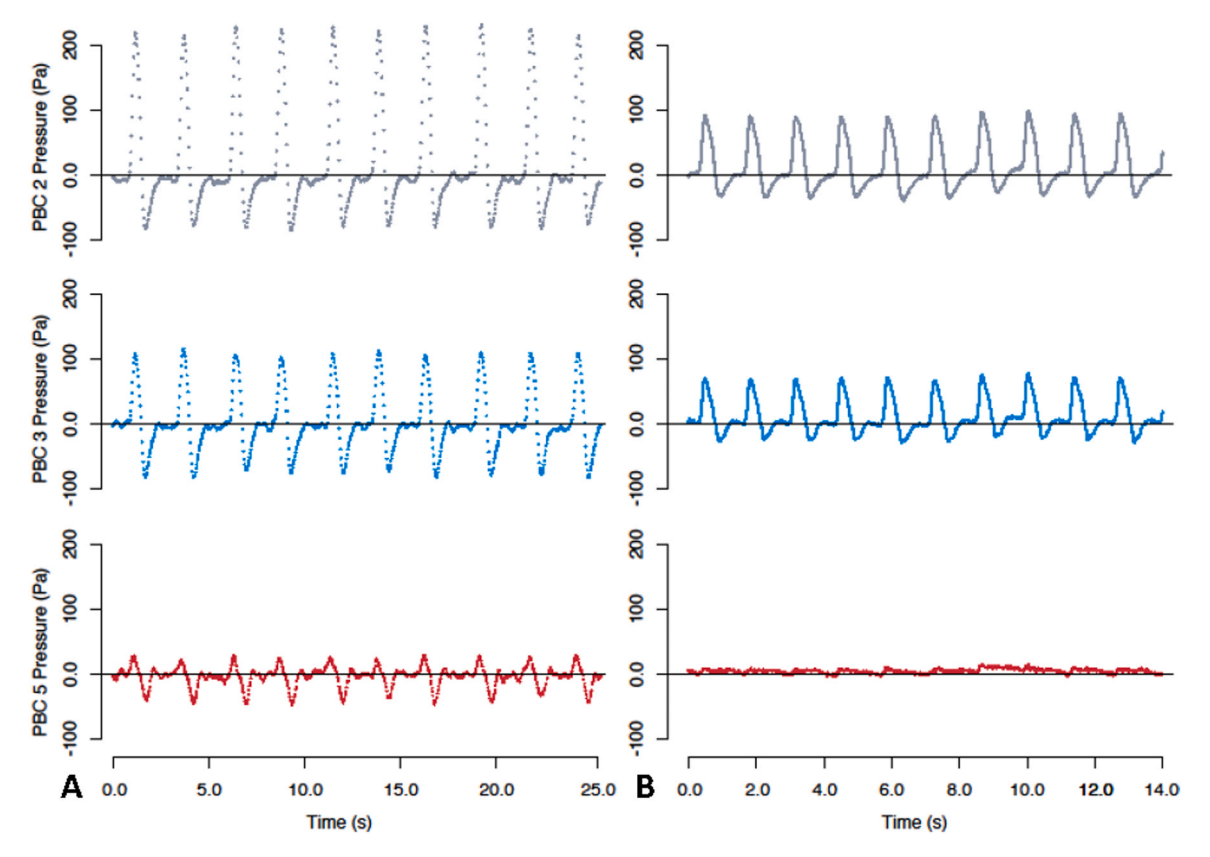
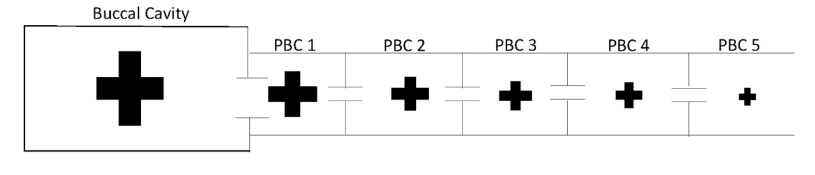


**Fig. 5. Different ventilatory modes of** *S. suckleyi*. Each panel represents a series of breaths collected from two different individuals. In both panels, the height of each peak indicates the magnitude of the pressure amplitude generated during each breath by each PBC. The area of the curve above zero represents the positive pressure "force" pump, while the area of the curve below zero represents the "suction" pump. Panel A shows a representative "active" pressure trace where PBC 5 is on, but pressure decreases anteriorly to posteriorly. Panel B shows a representative "quiet" case, where PBC 5 is not generating an amplitude.

Case 1: Active Mode



Case 2: Quiet Mode

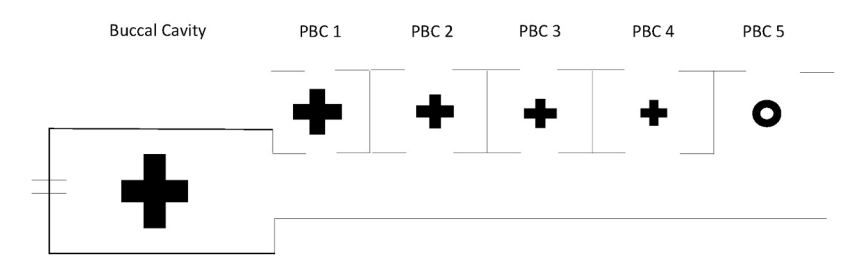


Fig. 6. Model for difference in activity of PBC 5. Modification to the model proposed by Hughes (1960b) to capture the variation in the pressures generated in PBC 5 during the ventilatory cycle in *Squalus suckleyi*. Depicted in both cases is the pressure pump phase of ventilation. In Case 1, the active mode, interbranchial resistance is equal amongst PBC chambers, such that there is a positive amplitude in each chamber and attenuation of pressure is due only to friction. In Case 2, the quiet mode, interbranchial resistance is increased via the closure of the gill flap at PBC 5, preventing water from entering the chamber.

change dramatically, potentially to achieve hydrodynamic crypsis. The most extreme example of this is in the angel shark (*Squatina japonica*) that ceases to use oral pumping during quiet breathing (Tomita et al., 2018). All gill slits may be activated in response to increased metabolic demand, such as the period following activity, like an increase in swimming speed resulting from escape from predators or the pursuit of prey (Lear et al., 2017). In cases where metabolic demand is increased, such as during swimming, it is likely that all PBCs perform at maximum pressure generation to increase ventilatory flow to sustain metabolism

(Piiper et al., 1977). Thus, we might expect each PBC to become more similar in overall pressure performance compared to the differences observed during rest in this study. Given PBC 5's increased length relative to the anterior four PBCs, it may accommodate a higher volume of flow during swimming; the specific changes of pressure generation by each PBC with increasing swimming speed in *S. suckleyi* are the subject of ongoing study by the authors.

We note at least two distinct ventilatory modes have been described: a quiet mode where PBC 5 appears to be purposefully inactive versus an

S. Arnette et al. Zoology 159 (2023) 126106

active mode when PBC 5 generates pressure. This behavioral modulation of the parabranchial chambers mirrors previously documented behavioral modulation of the oral cavity, such as the relative usage of the spiracle or oral opening during different ventilatory behaviors. The kinematic complexity of pump ventilation allows for modulation along many axes of kinematic variation, and the five paired parabranchial chambers of elasmobranchs offer even more opportunity for fine-tuned control of ventilatory hydrodynamics. One such example is observed in *Heterodontus portjacksoni* wherein the role of water intake, canonically associated with the orobranchial cavity, is shifted to the first parabranchial opening during periods of low oxygen tension (Grigg,1970). The model proposed by this study takes into account functional complexity of the parabranchial chambers that may allow sharks to respond to varying physiological demands and environments.

# **Declaration of Competing Interest**

The authors declare that they have no known competing financial interests or personal relationships that could have appeared to influence the work reported in this paper.

## Data availability

Data will be made available on request.

# Acknowledgements

This project was supported by NSF BIO 1852096 and 2000268 awarded to SCF. We thank Mo Turner, Kory Evans, Jackob Bueche, and Kristy Kull for assistance in catching dogfish. We also extend our gratitude to JoJo West and K Amacker for their help in data collection, as well as to Alice Gibb for her guidance. We are grateful to Friday Harbor Labs for equipment and facilities, and especially to Fred Ellis, Peggy Combs, and Dylan Crosby. Finally, we thank the two anonymous reviewers for their helpful comments.

# References

- Booth, J.H., 1978. The distribution of blood flow in the gills of fish: application of a new technique to rainbow trout (Salmo Gairdneri). J. Exp. Biol. 73 (1), 119–129. https:// doi.org/10.1242/jeb.73.1.119.
- Brainerd, E., Ferry-Graham, L., 2005. Mechanics of respiratory pumps. Fish Physiol. 23, 1–28. https://doi.org/10.1016/S1546-5098(05)23001-7.
- Dolce, J.L., Wilga, C.D., 2012. Evolutionary and ecological relationships of gill slit morphology in extant sharks. Bull. Mus. Comp. Zool. 161 (3), 79–109
- Ferry-Graham, L.A., 1999. Mechanics of ventilation in swellsharks, Cephaloscyllium ventriosum (Scyliorhinidae). J. Exp. Biol. 202, 1501–1510. https://doi.org/10.1242/ jeb.202.11.1501.
- Goto, T., Shiba, Y., Shibagaki, K., Nakaya, K., 2013. Morphology and ventilatory function of gills in the carpet shark family parascylliidae (Elasmobranchii, Orectolobiformes). Zool. Sci. 30 (6), 461–468. https://doi.org/10.2108/zsj.30.461.

- Grigg, G.C., 1970. Use of the first gill slits for water intake in a shark. J. Exp. Biol. 52 (3), 569–574. https://doi.org/10.1242/ieb.52.3.569.
- Hughes, G.M., 1960a. A comparative study of gill ventilation in marine teleosts. J. Exp. Biol. 37, 28–45. https://doi.org/10.1242/jeb.37.1.28.
- Hughes, G.M., 1960b. The mechanism of gill ventilation in the dogfish and skate. J. Exp. Biol. 37, 11–27. https://doi.org/10.1242/jeb.37.1.11.
- Kelly, M.L., Spreitzenbarth, S., Kerr, C.C., Hemmi, J.M., Lesku, J.A., Radford, C.A., Collin, S.P., 2021. Behavioural sleep in two species of buccal pumping sharks (Heterodontus portusjacksoni and Cephaloscyllium isabellum). J. Sleep. Res. 30 (3), 131–139. https://doi.org/10.1111/jsr.13139.
- Lear, K.O., Whitney, N.M., Brewster, L.R., Morris, J.J., Hueter, R.E., Gleiss, A.C., 2017. Correlations of metabolic rate and body acceleration in three species of coastal sharks under contrasting temperature regimes. J. Exp. Biol. 220 (3), 397–407. https://doi.org/10.1242/jeb.146993.
- Mecklenburg, C.W., Lynghammar, A., Johannesen, E., Byrkjedal, I., Christiansen, J.S., Dolgov, A.V., Karamushko, O.V., Mecklenburg, T.A., Møller, P.R., Steinke, D., Wienerroither, P.R., 2018. Marine fishes of the Arctic region. Conserv. Arct. Flora Fauna, Akure, Icel. Volume I.
- Muir, B.S., Buckley, R.M., 1967. Gill Ventilation in *Remora remora*. Copeia 3, 581–586. https://doi.org/10.2307/1442235.
- Mytilineou, C., Politou, C.-Y., Papaconstantinou, C., Kavadas, S., D'Onghia, G., Sion, L., 2005. Deep-water Fish Fauna in the Eastern Ionian Sea. Belg. J. Zool. 135 (2), 229–233.
- Piiper, J., Meyer, M., Worth, H., Willmer, H., 1977. Respiration and circulation during swimming activity in the dogfish Scyliorhinus stellaris. Respir. Physiol. 30, 221–239. https://doi.org/10.1016/0034-5687(77)90032-9.
- Popovic, N., Strunjak-Perovic, I., Coz-Rakovac, R., Barisic, J., Jadan, M., Persin Berakovic, A., Sauerborn Klobucar, R., 2012. Tricaine methane-sulfonate (MS-222) application in fish anaesthesia. J. Appl. Ichthyol. 28, 553–564. https://doi.org/ 10.1111/j.1439-0426.2012.01950.x.
- R Core Team, 2021. R: A Language and Environment for Statistical Computing. R
  Foundation for Statistical Computing, Vienna, Austria. (https://www.R-project.org/).
- Randall, D.J., 1970. Gas Exchange in Fish. In: Fish Physiology, vol. IV. Academic Press, New York.
- Roberts, J.L., 1975. Active branchial and ram gill ventilation in fishes. Biol. Bull. 148 (1), 85–105. https://doi.org/10.2307/1540652.
- Scheid, P., Hook, C., Piiper, J., 1986. Model for analysis of counter-current gas transfer in fish gills. Respir. Physiol. 64 (3), 365–374. https://doi.org/10.1016/0034-5687(86)
- Steen, J.B., Kruysse, A., 1964. The respiratory function of teleost gills. Comp. Biochem. Physiol. 12, 127–142. https://doi.org/10.1016/0010-406X(64)90168-9.
- Steffensen, J.F., Lomholt, J.P., 1983. Energetic cost of active branchial ventilation in the sharksucker, *Echeneis naucrates*. J. Exp. Biol. 103 (1), 185–192. https://doi.org/ 10.1242/jeb.103.1.185.
- Summers, A.P., Ferry-Graham, L.A., 2001. Ventilatory modes and mechanics of the hedgehog skate (*Leucoraja erinaceae*): testing the continuous flow model. J. Exp. Biol. 204, 1577–1587. https://doi.org/10.1242/jeb.204.9.1577.
- Tomita, T., Toda, M., Murakumo, K., 2018. Stealth breathing of the angelshark. Zoology 130, 1–5. https://doi.org/10.1016/j.zool.2018.07.003.
- Wegner, N.C., Graham, J.B., 2010. George hughes and the history of fish ventilation: from Du Verney to the present. Comp. Biochem. Physiol. Part A, Mol. Integr. Physiol. 157 (1), 1–6. https://doi.org/10.1016/j.cbpa.2010.03.004.
- Wegner, N.C., Chin Lai, N., Bull, K.B., Graham, J.B., 2012. Oxygen utilization and the branchial pressure gradient during ram ventilation of the shortfin mako, Isurus oxyrinchus: is Lamnid Shark-Tuna convergence constrained by elasmobranch gill morphology? J. Exp. Biol. 215 (1), 22–28. https://doi.org/10.1242/jeb.060095.
- Wegner, N.C., 2016. Elasmobranch Gill Structure. In: Shadwick, R.E., Farrell, A.P., Brauner, C.J. (Eds.), Physiology of Elasmobranch Fishes: Structure and Interaction with Environment, Vol 34A. Elsevier, pp. 101–151.